

How rapidly do the southern subtropical oceans respond to wind stress changes?

Darryn W. Waugh¹ and Thomas W N Haine¹

¹Johns Hopkins University

November 21, 2022

Abstract

The response time of the southern subtropical oceans to an increase in the wind stress is examined in a climate model perturbation simulation where there is an abrupt increase in the wind stress. The ocean response time is shown to vary among fields: The intensification of the gyres and vertical movement of isopycnals happens over 5-10 years, while the change in ideal age, temperature, and salinity in mode and intermediate waters occurs much slower, with the response time exceeding 100 years at depths of 500-1000 m. While the response time for ideal age is longer than that for the surface circulation it is notable that it is much younger than the ideal age itself. The different response times indicate that changes in the winds over the southern oceans and in the horizontal circulation / density structure will occur near simultaneously, but there may be a substantial lag in subsurface changes from wind changes and these may persist for decades even if no further changes in the winds occurs

20 **Abstract**

21 The response time of the southern subtropical oceans to an increase in the wind stress is
22 examined in a climate model perturbation simulation where there is an abrupt increase in the
23 wind stress. The ocean response time is shown to vary among fields: The intensification of the
24 gyres and vertical movement of isopycnals happens over 5-10 years, while the change in ideal
25 age, temperature, and salinity in mode and intermediate waters occurs much slower, with the
26 response time exceeding 100 years at depths of 500-1000 m. While the response time for ideal
27 age is longer than that for the surface circulation it is notable that it is much younger than the
28 ideal age itself. The different response times indicate that changes in the winds over the
29 southern oceans and in the horizontal circulation / density structure will occur near
30 simultaneously, but there may be a substantial lag in subsurface changes from wind changes
31 and these may persist for decades even if no further changes in the winds occurs.

32

33 **Plain Language Summary**

34

35 The time it takes properties of the southern hemisphere subtropical oceans to respond to changes
36 in the westerly winds blowing over the oceans is examined using a simulation of the climate
37 model in which the wind stress is abruptly increased. This idealized simulation enables the
38 response time to be easily quantified, and it is shown that there is a wide range of response times
39 among ocean properties. The increase in the horizontal circulation and vertical movement of
40 surfaces of constant density happens over around 5 years, whereas the response time of
41 temperature, salinity, and mean transit time within the ocean interior can exceed 100 years. This
42 means that while changes in the horizontal circulation will occur near simultaneously with
43 changes in the winds, there will be a substantial lag in changes in subsurface properties and these
44 properties will be insensitive to year-to-year variations in the winds.

45 **1 Introduction**

46 Changes in a wide range of characteristics of the southern oceans have been observed
47 over the last few decades, including changes in the heat and carbon content (e.g., Cai et al. 2010,
48 Le Quéré et al., 2007), the Antarctic circumpolar current (e.g., Boning et al 2008), strength of the
49 subtropical gyres (e.g., Roemmich et al. 2007, 2016), ventilation ages (e.g., Waugh et al. 2013,
50 Ting and Holzer 2017), and mode water properties (Gao et al. 2018). Many of these changes
51 have been linked to the intensification and poleward shift of the surface westerly winds over the
52 same period (e.g., Thompson et al. 2011, Swart and Fyfe 2012). However, while the above
53 ocean changes are qualitatively consistent with the expected response, it is difficult to attribute
54 the ocean changes to the wind stress changes because of a lack of a quantitative understanding of
55 the response of ocean properties to changes in wind stress.

56 One aspect where improved understanding is required is the transient nature of the ocean
57 response. While it is expected that different aspects of the oceans will respond to wind stress
58 perturbations over different time scales (e.g., there will be a slower response for tracers within
59 the ocean interior than the response of ocean surface circulation, just as it takes longer for
60 simulations of ocean tracers to reach equilibrium than for the surface circulation), how the
61 transient response differs between fields and spatially has not been quantified. This
62 quantification is important for both interpreting observed ocean changes and making projections
63 of future changes. For example, whether observed ocean changes should be linked with
64 simultaneous changes in wind stress or to the lagged or time-integrated change in wind stress
65 depends on the response time of the ocean property. This response time also determines how
66 long changes in the ocean persist after a change in the wind forcing depends on the response time
67 of the particular ocean property.

68 This latter issue is particularly important given past and projected changes in the wind
69 stress over southern mid-latitudes. Meteorological reanalyses show an increase and poleward
70 shift in the summer-time wind stress over southern mid-latitudes between 1970 and 2000, but
71 there has been little change in strength and latitude of peak summer winds since 2000 (Banerjee
72 et al. 2020). This ‘pause’ in trends is consistent with climate model simulations which show an
73 increase/poleward shift from 1975 to 2000 (due primarily to the formation of the ozone hole) and
74 then no trend from 2000 to ~2030 (as ozone hole stabilizes and any recovery is balanced by
75 continued growth of CO₂) (Barnes et al. 2014). It is unknown how quickly the oceans will
76 respond to this pause in wind stress trends, i.e., will the trends in ocean properties discussed
77 above also pause, or will there be a time lag and persistence of ocean trends even when no trends
78 in the wind stress?

79 Here we address the above questions by examining the transient response of the
80 subtropical oceans in a climate model simulation in which there is an abrupt increase in the wind
81 stress over the southern oceans. Numerous studies have examined the long-term response of the
82 ocean circulation, hydrography, and tracer distributions to an abrupt change in wind stress (e.g.,
83 Sijp and England 2008, Farneti et al. 2010, Gent and Danabasoglu 2011, Spence et al. 2014,
84 Waugh 2014, Downes et al. 2017, Hogg et al. 2017, Waugh et al. 2019), but little attention has
85 been paid to time scales for these responses. Here we quantify, for the first time, the transient
86 response of multiple aspects of the southern subtropical oceans to an increase in wind stresses.
87 Specifically, we examine the response of the barotropic transport stream function, density, ideal
88 age, temperature, and salinity fields. We consider the ideal age as it equals the mean time for
89 transport from the surface to an interior location, a fundamental property of the ocean transport.

90 Also, recent studies have shown changes in the age of southern mode waters inferred from
91 observations (e.g., Waugh et al 2013, Tanhua et al. 2013, Ting and Holzer 2015, Fine et al.
92 2017), and suggested that this is due to changes in the wind stresses. However, quantification of
93 the transient response of the age is required to test this suggestion. Finally, changes in age can
94 provide information on (be used to estimate) changes in oceanic anthropogenic carbon, heat, and
95 oxygen (e.g. Russell et al. 2016).

96 The model experiments and analysis methods are described in the next Section. In
97 Section 3 we briefly discuss the long term (100 year) response of the fields, and then in Section 4
98 examine the evolution and responses times. In Section 5 linear response theory is used to
99 estimate the response of the fields for arbitrary time-varying changes in the wind stress.
100 Concluding remarks are in the final section.

101

102 **2. Model Experiments**

103 We examine the output from a wind-stress perturbation simulation performed in the
104 Community Climate System Model version 4 (CCSM4) (Gent and Danabasoglu 2011).
105 CCSM4 is a fully coupled atmosphere-ocean model as documented in Gent et al. (2011). The
106 ocean component has 60 vertical levels, with horizontal resolution around 1° . Mesoscale eddies
107 are not resolved and are parameterized using a Gent and McWilliams eddy parameterization
108 with a coefficient k that is a function of space and time.

109 In the wind-stress perturbation examined here the wind stress forcing is multiplied by the
110 factor 1.5 south of 35°S from that in a long preindustrial control run (which will be referred to
111 simply as the “control” run). This results in increases of the maximum zonally averaged zonal
112 wind stress from 0.19 to 0.28 N m^{-2} but does not change the latitude of the maximum wind stress
113 (**Figure 1a**). This perturbation is not meant to represent the past changes in southern winds,
114 which involve changes in location as well as strength of peak winds as well as zonal variations in
115 the wind changes, but rather to provide a clean experiment to isolate the response to an increase
116 in wind stress.

117 The wind-stress perturbation simulation is run for 100 years, and the control simulation is
118 also extended for 100 years. There is interannual variability in the wind stresses in both the
119 control and perturbation simulations, but the magnitude of this variability is much less than the
120 difference in wind stress between simulations (e.g., the interannual standard deviation of the
121 maximum wind stress in the control simulation is 0.01 N m^{-2} is much smaller than the mean
122 difference of 0.09 N m^{-2} between simulations).

123 As described in Gent and Danabasoglu (2011), the increased zonal wind stress in the
124 perturbation simulation does not directly affect the atmosphere-to-ocean heat and freshwater
125 fluxes. But there is an indirect effect on the coupled system through changes to the sea surface
126 temperature caused by the stress change, which results in changes in air-sea fluxes between
127 simulations. The differences in these fluxes between simulations are small, however: the large-
128 scale patterns of the fluxes are the same, and the differences that occur are generally associated
129 with small shifts in localized regions of high fluxes.

130 We consider the response of several different fields: The barotropic stream function
131 (BSF), potential density referenced to 2000 dbar (σ_2), temperature (T), salinity (S), ideal age
132 (Γ). The ideal age is a tracer that yields, in the limit of long times compared to the circulation,
133 the mean time since water last made surface contact (e.g., England 1995, Hall and Haine 2002).

134 The response of a given field is calculated as the difference between the perturbation and
 135 control simulations evaluated at the same time. To quantify the time scale of the response we fit
 136 the time series of the specified field with the function

$$137 \quad R(t) = R_0(1 - e^{-t/\tau}) \quad (1)$$

138 where R_0 is the steady-state response and τ the e-folding time of the response (which we refer
 139 to as the response time). The steady-state response R_0 of some of the fields considered has
 140 been examined in previous studies (Gent and Danabasoglu 2011, Waugh 2014), but the
 141 response time τ has not. The response time τ should not be confused with the ideal age, and, as
 142 will be shown below, τ is generally not the same as the ideal age Γ .

143 **3. Long-term Response**

144 Before examining the temporal variation in fields of interest we briefly examine the
 145 response 100 years after the perturbation is applied. The changes in σ_2 , Γ , and T after 100 years
 146 in these simulations have been examined in more detail in Gent and Danabasoglu (2011) and
 147 Waugh (2014). **Figure 1b-h** shows the response (difference between the two simulations) of
 148 the BSF, σ_2 , Γ , T , and S fields at 100 yr.

149 There is an increase in the magnitude of the BSF (more negative BSF) throughout most
 150 of the subtropical oceans (**Figure 1b**), which corresponds to an intensification of the subtropical
 151 gyres. As shown in previous studies (e.g., Saenko et al. 2005, Cai 2006, Cai and Cowen 2007,
 152 Waugh et al 2019), this response is consistent with Sverdrup balance, i.e., there is an increase in
 153 the wind stress curl north of 50°S and within this region the magnitude of the BSF increases.

154 The change in wind stress curl also leads, via Ekman pumping, to changes in the density
 155 structure (**Figure 1c**). There is a shoaling (upward movement) of isopycnals south of 45°S
 156 where the wind stress curl decreases, and deepening (downward movement) of isopycnals north
 157 of 45°S, except near the surface. This movement of isopycnals corresponds to a steepening
 158 (increase in horizontal gradients) of isopycnals across the Antarctic circumpolar current. Note,
 159 although the simulations do not resolve eddies, the eddy parameterization coefficients are a
 160 function of space and time, which results in partial eddy compensation (Gent and Danabasoglu
 161 2011, Gent 2016).

162 As shown in Waugh (2014), there is a significant decrease in ideal age (i.e. age
 163 decrease is much larger than the interannual variability and trend of the control run) within
 164 mode and intermediate waters ($35.5 \text{ kg/m}^3 < \sigma_2 < 36.5 \text{ kg/m}^3$) in the CCSM4 wind stress
 165 perturbation, see **Figure 1d**. It is notable that the spatial structure and magnitude of the age
 166 response is very similar to that for the abrupt increase wind perturbation in the 0.25° ocean-sea
 167 ice model simulation examined in Waugh et al (2019). In both simulations the peak decrease
 168 in age exceeds 50 years and occurs around 35°S and 1000-1500 m depth. The agreement
 169 suggests that a coarse-resolution climate model with parameterized eddies (e.g., CCSM
 170 simulation considered here) may produce a similar change in ideal age as a higher resolution
 171 eddy permitting model.

172 The change in age is due to both transport along isopycnals and movement of isopycnal
 173 surfaces. We decompose the change in age at fixed depth (the “total” change) into the change
 174 due to transport along isopycnals (“isopycnal” change”) and that due to the wind-driven
 175 movement of isopycnals (“heave”; Bindoff and McDougall (1994)). The isopycnal change is

176 determined by calculating the change in age at fixed density (for each latitude) and then
 177 mapping this to depth space using the the control density distribution. The change due to heave
 178 is calculated by mapping the perturbation age in density space into depth space using the
 179 control density distribution, and then taking the difference from the control age in depth space.

180 **Figures 1e,f** show the heave and isopycnal change in age. The spatial structure of the
 181 age change differs between processes: Heave produces an increase in age between 45 and 60 °S
 182 but a decrease between 20 and 40 °S (consistent with changes in density shown in **Figure 1c**),
 183 whereas isopycnal change produces a decrease throughout mode and intermediate waters. The
 184 largest changes in age at fixed depth (**Figures 1d**) occur in regions where heave and isopycnal
 185 change cause the same sign change in age (e.g. both cause a decrease in age around 1000m,
 186 35°S), while the smallest change occurs in regions where they oppose each other (e.g. 200-
 187 1000m, 50°S). The relative role of changes in age due to heaving and isopycnal transport
 188 shown in **Figure 1** is again consistent with the eddy-permitting simulations analyzed in Waugh
 189 et al (2019).

190 The increase in the wind stress also results in changes in the temperature and salinity
 191 fields. As shown in **Figures 1g,h** there is an increase in both zonal-mean T and S through
 192 most of mode and intermediate waters. The spatial structure of the response is somewhat
 193 different between the two fields: The maximum total change in T occurs around 1000 m
 194 between 30 and 40°S, whereas maximum increase in S occurs further south and at the surface
 195 (above 500 m and around 55°S). This difference in spatial structure is because the impact of
 196 heave varies between fields. As there are only weak vertical S gradients (contours in **Figure**
 197 **1h**) the movement of isopycnals (heave) has only a small impact on S. In contrast there are
 198 strong vertical gradients of T through mode and intermediate water, and like age, there are
 199 substantial changes in T due to heave. The pattern of the isopycnal changes in T and S are the
 200 same (as they must be), with both fields increasing in mode and intermediate waters with the
 201 maximum increase nearer the surface around 55°S (see contours in **Figures 3d** below).

202

203 **4. Response Time**

204 We now examine the evolution of the above fields, and how long it takes the fields to
 205 reach a new statistically-steady state following the abrupt wind change. We first consider the
 206 response of the BSF. **Figure 2a** shows that the intensification of the gyres (decrease in minimum
 207 BSF) happens rapidly, with the vast majority of the decrease in the minimum BSF in each basin
 208 occurring within the first 10 years. Fitting the minimum BSF time series with equation (1) yields
 209 response times $\tau \sim 3-6$ years. Similar short response time scales are also found for individual
 210 locations within the subtropical gyres (not shown). This ~ 5 year spin-up time is similar to that in
 211 previous studies examining the response of subtropical gyres to changes in wind stresses (e.g.,
 212 Deser et al.1999, Thomas et al. 2014), which linked the response time to the basin crossing time
 213 of baroclinic Rossby waves. Note that in the presence of topography there is an interaction
 214 between baroclinic and barotropic modes which results in a slow adjustment of the barotropic
 215 mode on the time scale of the baroclinic modes (e.g., Anderson and Killworth 1977, Anderson et
 216 al. 1979).

217 There is also generally a fast response in the density structure, with the upward or
 218 downward movement of isopycnals occurring primarily in the first 20 years. This is illustrated
 219 in **Figure 2b** for three locations with initial $\sigma_2 = 36.0 \text{ kg/m}^3$ (see diamonds in **Figure 1**). At the

220 southern-most location shown (49°S) there is an increase in σ_2 over the first 20 years
 221 ($\tau \sim 10$ yrs), while at the northern-most location (36°S) there is a rapid decrease ($\tau \sim 5$ yrs). At
 222 43°S there is only a weak change in σ_2 (consistent with **Figure 1c**) and $\tau \sim 90$ yrs. For latitudes
 223 between 30°S and 55°S the response time is 5-10 yrs except in the regions where there is
 224 little change in density, see **Figure 3a**. Note, in **Figure 3a** values are not shown if equation (1)
 225 is a poor fit to the response (i.e., if the root-square mean difference divided by the mean change
 226 exceeds two). North of 30°S, where there is no change in the wind stress (**Figure 1a**), the
 227 decrease in σ_2 at fixed depth occurs more slowly, with a roughly linear increase over the 100
 228 years of the perturbation simulation (not shown). This slow deepening of isopycnals is
 229 consistent with theory and idealized modeling showing a centennial timescale for deepening of
 230 the global pycnocline due to interactions between the Southern Ocean and northern basins
 231 (Jones et al. 2011; Allison et al. 2011).

232 The response time of Γ varies with latitude and depth, and also between isopycnal and
 233 heave change. This is illustrated in **Figure 2c-e** which shows the time series of the change in
 234 zonal-mean Γ for the three locations discussed above, for the total, heave, and isopycnal change,
 235 respectively. As expected, the evolution (and response time) of the change in age due to heave is
 236 very similar to that for the change in density.

237 There is a large variation in τ for the isopycnal change in age (**Figures 2e, 3d**). Near the
 238 surface τ is less than 5 years but τ increases with depth, and exceeds 100 yrs at deep, northern
 239 latitudes. The longer response time of the ideal age compared to that of the BSF and density
 240 occurs because the BSF and density response times are controlled by wave dynamics (most
 241 likely the basin crossing time of Rossby waves) whereas the ideal age response is controlled by
 242 the advection and mixing of tracers from the surface to the interior location which occur over
 243 longer time scales.

244 There is generally a monotonic increase in τ with more equatorward locations along an
 245 isopycnal, with τ increasing roughly linearly with distance from the outcrop for 10-15° degree
 246 north of an outcrop, see **Figure 4a**. The ideal age also increases roughly linearly with distance
 247 from the outcrop but more rapidly than τ , see **Figure 4b**. This means that τ is much younger
 248 than Γ , see **Figure 4c**. This is somewhat surprising as the ideal age is the mean time for
 249 transport from the surface to interior location, and it might be expected that the time to respond
 250 to changes in the circulation will be similar to this mean transport time. In addition, for the
 251 simple case of uniform advection with no mixing the time for the ideal age (which equals the
 252 distance from source divided by advection speed) to come to a new steady state after an abrupt
 253 increase in flow speed is equal to the age in the new state, i.e. $\tau = \Gamma$.

254 Why the response time of the age in mode and intermediate waters in the CCSM
 255 perturbation simulation is much less than the age itself is unknown. Possible insights into the
 256 difference between t and Γ come from comparison of the slopes of their relationships with
 257 latitude. The slope of the latitude- τ relationships are around 0.2-0.3 cm/s (solid lines in
 258 **Figures 4a**). This “propagation” speed is of similar order to the time-mean meridional flow in
 259 the gyre (away from the western boundary current), possibly suggesting that τ may be
 260 determined primarily by the advective timescale. There is a smaller slope of the latitude-
 261 Γ (~ 0.01 - 0.04 cm/s; solid lines in **Figures 4b**), corresponding to slower “propagation” of Γ .
 262 Thus Γ is larger than the advective time, consistent with mixing playing a major role in

263 determining Γ . This suggests the age response time is determined primarily by the advection
 264 of young waters to a given location, whereas the ideal age is influenced also by mixing with
 265 older (recirculated) waters. Further analysis is required to determine if this indeed the case, but
 266 is beyond the scope of this work.

267 The transient response of Γ at fixed depth differs between regions with differing
 268 balances between heave and isopycnal changes (**Figures 2c, 3c**). Between 30 and 40°S where
 269 both heave and changes in along-isopycnal transport cause a decrease in age the response time
 270 of Γ at fixed depth is generally less than that due to isopycnal transport, as the deepening of
 271 isopycnals (and decrease in age at fixed depth) occurs more rapidly than the decrease due to
 272 isopycnal transport. South of 40°S the isopycnals shoal and the age change due to heave
 273 opposes that due to along-isopycnal transport, and there is generally only a small change in age
 274 at fixed depth after 100 years (Figure 1). The time to reach the 100-yr change increases with
 275 depth, but for many locations the equation (1) is a poor fit for the response and τ cannot be
 276 defined using this relationship. This occurs because the initial (~5-10 yr) increase in age due to
 277 shoaling is of similar magnitude to the long time decrease due to along-isopycnal transport.
 278 The response in this region could be fit by a two-time scale equation (i.e. a second exponential
 279 term in equation 1) but we have not done this as the change age in this region is very small
 280 (Figure 1).

281 The response times for T and S share similarities with that for Γ : The response times for
 282 T and S vary spatially (latitude and depth), between isopycnal and heave change, and are
 283 generally much slower than the BSF and density responses. The timescale for heave changes in
 284 T and S are generally less than 5 years and similar to that for age (and vertical movement of
 285 isopycnals), and are not shown. However, the response time τ for isopycnal changes in T and S
 286 is in most regions greater than τ for isopycnal changes in age, see **Figures 2 and 3**. As the
 287 evolution of T and S on isopycnal surface is the same, we only show the evolution and response
 288 time for T in **Figures 2 and 3**.

289 While isopycnal changes (decreases) in ideal age occur because of more rapid surface to
 290 subsurface transport, this is not the primary cause of the isopycnal increases in T or S. As both T
 291 and S increase with depth along isopycnals, more rapid along-isopycnal transport would bring
 292 lower tracer values to depth and cause a decrease in subsurface T and S, and not the increases in
 293 T and S. Instead, the primary cause is increases in mixed layer T and S where the $\sigma_2 = 35.5$ - 36.5
 294 kg/m^3 isopycnal surfaces outcrop (55-65°S). The increases in near-surface T and S occur within
 295 the first 5 years (see **Figure 5**), and are consistent with increases in the northward Ekman flow
 296 and upwelling in subpolar regions from increased wind stress (e.g., Ferreira et al. 2015). These T
 297 and S anomalies then propagate along isopycnals into subtropical mode/intermediate waters. As
 298 the ideal age is set to zero in the surface layer, this process does alter the ideal age in
 299 mode/intermediate waters.

300 Although the propagation of larger mixed layer T and S into the interior is likely the
 301 major cause of the isopycnal changes in these tracers, the increase in the rate of transport
 302 (decrease in ideal age) may still play a role. For example, there are only small changes in T and
 303 S along the isopycnals where the largest decreases in age occur ($\sigma_2=36.5$ - 37.0 kg/m^3), possibly
 304 because of cancelation between increased mixed layer values and more rapid along-isopycnal
 305 transport into the interior.

306

307 5. Linear Response Functions calculations

308 The wind stress perturbation considered above is idealized, and the response cannot be
 309 directly compared with observations. However, assuming a linear response, the temporal
 310 evolution of a given field (e.g. BSF, age) from an abrupt wind-stress perturbation can be used
 311 together with “linear response function” theory to estimate the temporal evolution of the field
 312 for arbitrary time-varying changes in the wind stress.

313 If $R(t)$ is the linear transient response of a system variable Φ to a step function increase at
 314 time $t=0$ in a specified forcing, then the linear response of the variable Φ to arbitrary forcing $F(t)$
 315 (with $F=0$ for $t<0$) is (e.g., Hasselmann et al. 1993)

$$\Phi(t) = \int_0^t R(t-t') \frac{dF}{dt'}(t') dt' .$$

2)

316 Thus once R is known the change in variable Φ for any time variation in the forcing can be
 317 determined from (2). This approach has been used to examine the response of atmospheric
 318 surface temperatures to increases in CO_2 (e.g., Hasselmann et al. 1993) and more recently the sea
 319 surface temperature response to increases in CO_2 or ozone depletion (e.g. Marshall et al. 2014).

320 Here we will apply (2) to the wind-stress perturbation experiment, and examine the
 321 response of ocean fields to different temporal variations in the magnitude of the wind stress. In
 322 this case the wind-stress corresponds to the forcing F , and the time series of ocean field (BSF, Γ ,
 323 T , S , etc) in the abrupt perturbation simulations is, when appropriately scaled, equal to the
 324 response function R . Equation (2) is then used to estimate the change in ocean field for arbitrary
 325 temporal variations in the wind stress perturbation. A potential issue with this calculation is the
 326 assumption of linearity. However, analysis of simulations with an increase, a shift, and
 327 combined increase and shift of winds in Waugh et al (2019) suggest the response of the age in
 328 mode and intermediate waters is close to linear.

329 As discussed in the Introduction, observations and models indicate an intensification and
 330 poleward shift of the summer wind stress over the last few decades of the 20th century, but a
 331 pause, or even slight reversal, in these trends since around 2000 (Banerjee et al. 2020, Barnes et
 332 al. 2014). Given this we consider the idealized case where there is a linear increase in the
 333 magnitude of the wind stress from 1970 to 1999, followed by 30 years (2000-2029) with no
 334 change in the wind stress (thin lines in **Figure 6a**). This could be considered an idealization of
 335 the response to the formation of the Antarctic ozone hole and then stabilization. To see the
 336 impact of year-to-year variations we include a small oscillatory perturbation with period of 5
 337 years to these trends (thick curve in **Figure 6a**).

338 The simulated response of specific fields in CCSM4, such as shown in **Figure 2**, can be
 339 used to estimate the response functions $R(t)$ in the convolution (2). Rather than using the
 340 simulated response we consider for simplicity $R(t)$ of the idealized form of equation (1), with τ
 341 varying between 5 and 100 yrs (**Figure 6b**). This $R(t)$ can be used to estimate the response of
 342 different fields (at different locations). For example, $\tau = 5$ yrs is representative of change in the
 343 BSF, density, and near surface age, T and S , while $\tau = 50$ and 100 yrs are representative of
 344 change in age, T and S at mid-depths.

345 **Figure 6c** shows the response to the wind stress changes shown in **Figure 6a** for the
 346 different response functions in **Figure 6b**. There is a decrease with time for all τ , but (i) the
 347 amplitude of the 5-year variations and (ii) the longer term rate of decrease varies dramatically
 348 with τ . Only for $\tau = 5$ yrs are there noticeable oscillations about longer term decrease and even
 349 then the amplitude is much less than for the wind stress. In other words, for response times
 350 around and larger than $\tau = 10$ yrs the response is insensitive to variations short term (5 year or
 351 less) variations in the wind stress.

352 For $\tau = 5$ yrs (black curve in **Figure 6c**) the response in 2000 is ~85% of the equilibrium
 353 response and there are only very small changes after ~2010. In contrast, for $\tau = 50$ yrs (blue
 354 curve in **Figure 6c**) there is a significant delay in the response: The response in 2000 is only
 355 ~25% of the equilibrium response, and by 2030 it is still on ~60% (i.e. the field is still decreasing
 356 30 years after wind stress stopped increasing). In fact, it will not be until 2100 that response is
 357 90% of equilibrium response.

358 The calculations in **Figure 6c** suggest that the BSF will have essentially reached its full
 359 response to the pre-2000 trends in wind stress by ~2010 and will not change (due to wind stress
 360 changes) over the next few decades. However, the mid-depth age, T and S within mode /
 361 intermediate waters will still be responding in the early 2000s and will continue to change for 3
 362 or more decades even without a systematic change in the wind stress over this period, i.e. the
 363 impact of the wind stress trends at the end of the 20th century on mid-depth ocean properties
 364 could persist until the middle or even end of this century.

365 This smoothed, lagged response has important consequences for interpreting (inferring
 366 the cause of) observed changes in ocean properties. First, observed changes in subsurface fields
 367 should not be linked with simultaneous changes in wind stress but rather with a time-integrated
 368 (weighted) change in the wind stress. Second, it is possible there could a substantial decrease in
 369 the age (or increase in T and S) over a period with no trends in wind stress or BSF, which could
 370 be mistakenly interpreted as indicating trends in age, T and S are unrelated to wind stress of BSF
 371 changes.

372 Equation (2) provides insight into how to compare subsurface ocean changes with
 373 changes in the wind stress (i.e., to assess whether ocean changes are consistent with the wind
 374 stress changes). Differentiation of equation (2) yields

$$\frac{d\Phi}{dt}(t) = \int_0^t G(t-t') \frac{dF}{dt'}(t') dt', \quad (3)$$

375 where $G=dR/dt$ (note, G differs from the passive tracer transit time distribution). For $R(t)$ of the
 376 form (1) we have $G(t) = (R_0/\tau)e^{-t/\tau}$. Equation (3) implies a low-pass filter for changes in Φ
 377 compared to changes in F . A change (trend) in ocean property Φ (i.e., BSF, Γ , T, S) should then
 378 be compared with the time integral of the change (trend) in wind stress (F in equation 3) using
 379 weighting function G . For fields with a short response time τ (i.e. BSF) the integral (3) makes
 380 only a small difference and $d\Phi/dt \sim dF/dt$, but for $\tau \sim 20$ -100 yrs there is a large difference in
 381 temporal variation of Φ and F (as shown in Fig. 4). In the latter case, the interior fields will be
 382 insensitive to interannual and 3-5 year variations (such as ENSO) in the wind stress (because of
 383 the decadal smoothing). In addition, any respond to wind stress changes will be delayed by
 384 decades.

385

386

6. Conclusions

387

388

389

390

391

392

393

394

395

396

397

398

Analysis of an idealized wind-stress perturbation experiment indicates that the response of the southern subtropical oceans to an increase in the surface winds occurs over multiple time scales, and varies among ocean properties. There is a relatively rapid (5-10 year) intensification of the subtropical gyres and deepening / shoaling of isopycnals in response to an increase in the surface winds. However, the decrease in age and increase in temperature and salinity in mode waters is generally much slower, with response time increasing from order 5 years near the surface to over 100 years at depths of 500-1000 m. The changes in sub-surface age, T and S at fixed depth occur because of changes in isopycnal depth (heaving), along-isopycnal transport, and (for T and S) changes in mixed layer properties which get transported into the interior. These processes occur on different time scales, resulting in a multi-time scale response for age, T and S. The time scale for along-isopycnal transport is much longer than for heave or mixed layer properties, and generally dominates the response time for age, T and S at fixed depth.

399

400

401

402

403

404

405

406

407

A slower response for subsurface tracer properties than the gyre circulation is not a surprise, but it is notable that the response time for the ideal age is much less than the ideal age itself. It might be expected that the response time is similar to the ideal age, as the ideal age is the mean time for transport from the surface to interior location. However, this is not the case for the age response in mode and intermediate waters to an increase in the wind stress. Analysis of the increase of ideal age and its response suggests the age response time is determined primarily by the advection of young waters to a given location, whereas the ideal age is much more strongly influenced by mixing with older (recirculated) waters to the location. Further research is required to determine if this is the case.

408

409

410

411

412

413

We have focused here on changes within the subtropical oceans within the first 100 years (the length of the simulation), but there are also changes outside this region. This includes the deep waters forming around Antarctica as well as the rest of the oceans. As mentioned in Section 4, there is a slow deepening of isopycnals north of 30°S, consistent with a centennial timescale response of the global pycnocline and meridional overturning circulation (Jones et al. 2011; Allison et al. 2011).

414

415

416

417

418

419

420

421

422

423

424

The range of time scales for the response of different properties within the subtropical oceans to changes in the wind stress has consequences for the interpretation of observations. First, observed changes in subsurface fields should not be linked with simultaneous changes in wind stress but rather with a time-integrated (weighted) change in the wind stress (e.g. equation 3). For example, changes over a decade in the ideal age in mode waters should not be compared just with the wind stress changes over this period, but with changes over longer, multi-decadal period. Further, as the time scale of this weighting varies between fields and locations if there is a change in wind stress trends this may be observed in fast responding aspects of the oceans (e.g. horizontal circulation or density structure) but not in other properties (e.g., age, T and S in mode waters). This could mistakenly be taken to indicate that the changes in different properties are not driven by the same process.

425

426

427

428

The multi-decadal time scales for the subsurface response to changes in the wind stress also has consequence for current and projections of further changes. First, the subsurface fields will not be sensitive to less than decadal variations (e.g. ENSO) in the wind stress. Further, there will generally be a large (decades) lag between projected changes in wind stress and

429 changes in subsurface fields. For example, wind-driven trends in age, T, and S in interior
 430 mode/intermediate waters may continue for several decades even if there is pause in the
 431 intensification and poleward shift of the summer wind stress (Banerjee et al. 2020, Barnes et al.
 432 2014). This complicates attribution of observed changes in southern ocean mode waters to
 433 different natural and anthropogenic processes.

434 We plan to use these ideas in a comparison of repeat measurements of CFCs and SF₆ and
 435 changes in westerly winds over the southern oceans. Previous studies have analyzed
 436 measurements of these tracers made in the early 1990s and mid 2000s, and shown a decrease in
 437 ages within sub-Antarctic mode (e.g., Waugh et al 2013, Tanhua et al. 2013, Ting and Holzer
 438 2015, Fine et al. 2017). Additional measurements have been made along the same ocean sections
 439 in the last few years, which allows the opportunity to also estimate the change in age from mid
 440 2000s to mid-late 2010s. The evolution of age at different depths can then be compared with
 441 time-integrated changes in winds to test whether the changes in age can be attributed to the wind
 442 changes.

443 **Acknowledgments**

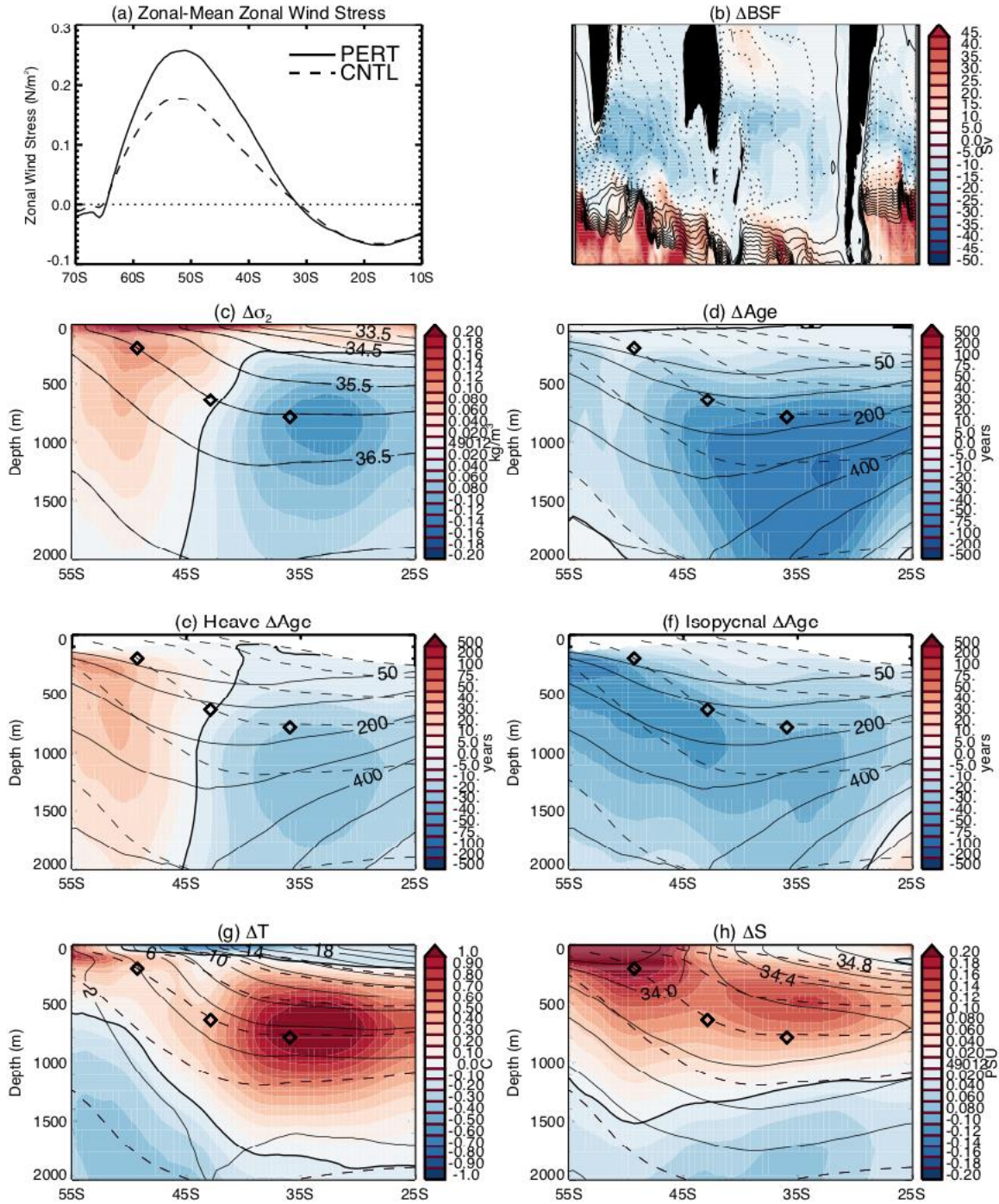
444 We thank P. Gent, G. Danabasoglu, F. Bryan and M. Long for discussions and advice regarding
 445 the CCSM4 simulations; and A Hogg for helpful discussions and comments on the manuscript.
 446 The CCSM4 data presented is archived on the Johns Hopkins University Data Archive at
 447 <https://archive.data.jhu.edu/dataverse/>.

448 **References**

- 449 Allison, L.C., Johnson, H.L. & Marshall, D.P. (2011), Spin-up and adjustment of the Antarctic
 450 Circumpolar Current and global pycnocline. *Journal of marine research*, 69(2-3), pp.167-189.
- 451 Anderson, D. L. T., & Killworth, P. D. (1977), Spin-up of a stratified ocean, with topography.
 452 *Deep-Sea Res.*, 24, 709–732.
- 453 Anderson, D.L., Bryan, K., Gill, A.E. & Pacanowski, R.C. (1979), The transient response of the
 454 North Atlantic: Some model studies. *Journal of Geophysical Research: Oceans*, 84(C8), 4795-
 455 4815.
- 456 Banerjee A, JC Fyfe, L. M Polvani, & D.W. Waugh (2020), A pause in Southern Hemisphere
 457 circulation trends due to the Montreal Protocol, *Nature* **to appear**.
- 458 Barnes, E.A., Barnes, N.W. & Polvani, L.M. (2014), Delayed Southern Hemisphere climate
 459 change induced by stratospheric ozone recovery, as projected by the CMIP5 models. *Journal of*
 460 *Climate*, 27, 852-867.
- 461 Bindoff, N. L., & T. J. Mcdougall, 1994: Diagnosing climate change and ocean ventilation using
 462 hydrographic data. *J. Phys. Oceanogr.*, 24, 1137–1152.
- 463 Boning, C. W., Dispert, A., Visbeck, M., Rintoul, S. R. & Schwarzkopf, F. U. 2008: The
 464 response of the Antarctic Circumpolar Current to recent climate change. *Nature Geosci.* 1, 864-
 465 869.
- 466 Cai, W., Cowan, T., Godfrey, S., & Wijffels, S. 2010: Simulations of processes associated with
 467 the fast warming rate of the southern midlatitude ocean. *J. Climate*, 23, 197-206.

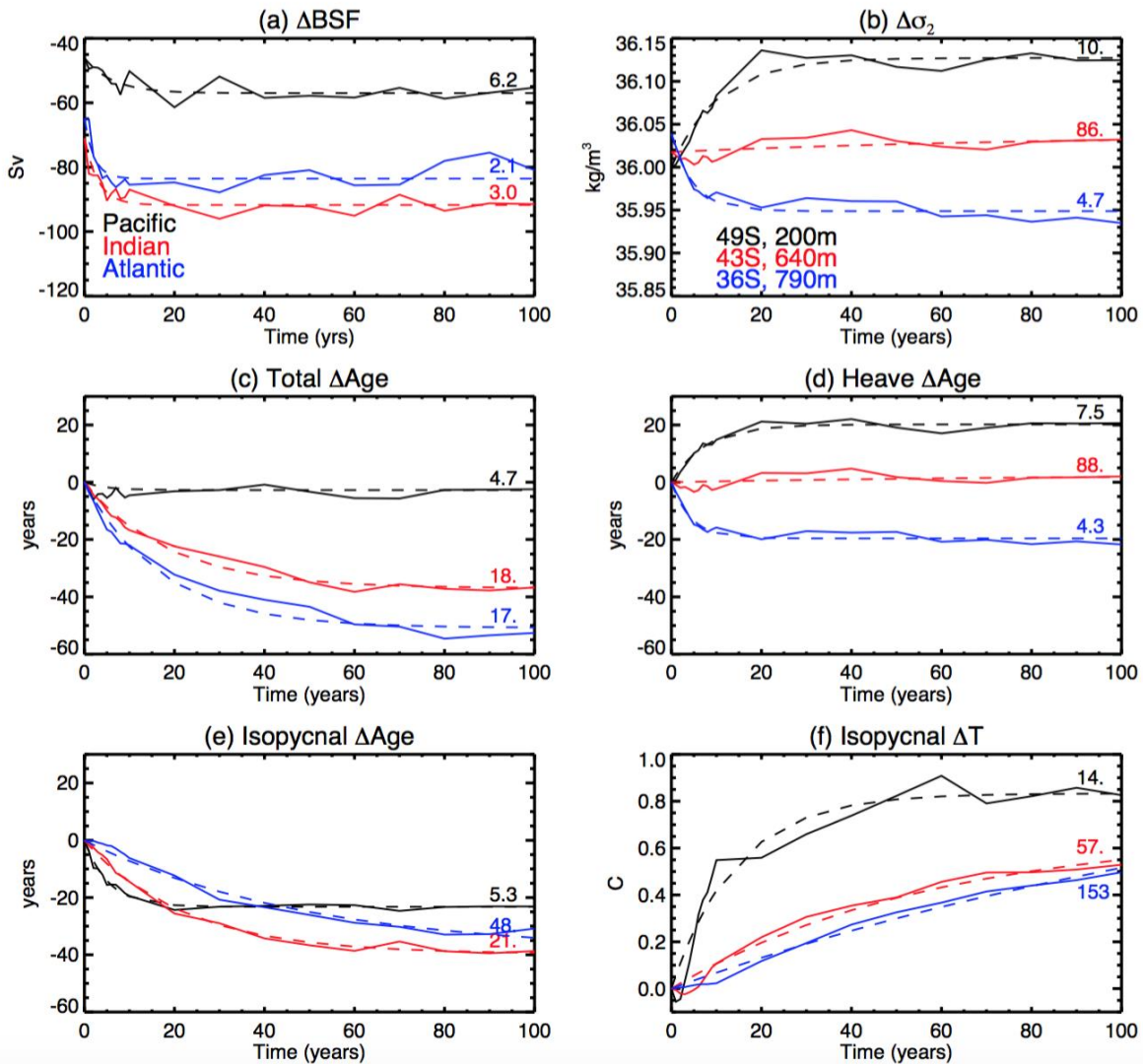
- 468 Deser, C., Alexander, M.A. & Timlin, M.S., 1999: Evidence for a wind-driven intensification of
469 the Kuroshio Current Extension from the 1970s to the 1980s. *Journal of Climate*, 12, 1697-1706.
- 470 Downes, S. M., C. Langlais, J. P. Brook, & P. Spence, 2017: Regional impacts of the westerly
471 winds on Southern Ocean Mode and Intermediate Water subduction. *J. Phys. Oceanogr.*, 47,
472 2521–2530.
- 473 England, M.H., 1995: The age of water and ventilation timescales in a global ocean model. *J*
474 *Phys. Oceanogr.*, 25, 2756-2777.
- 475 Farneti, R, T. L. Delworth, A. J. Rosati, S. M. Griffies, & F. Zeng, 2010: The role of mesoscale
476 eddies in the rectification of the Southern Ocean response to climate change. *J. Phys. Oceanogr.*,
477 40, 1539–1557.
- 478 Ferreira, D., J. Marshall, C. M. Bitz, S. Solomon, & R. A. Plumb, 2015: Antarctic Ocean and sea
479 ice response to ozone depletion: A two-time-scale problem. *J. Climate*, 28, 1206–1226.
- 480 Fine, R.A., Peacock, S., Maltrud, M.E. and Bryan, F.O., 2017. A new look at ocean ventilation
481 time scales and their uncertainties. *Journal of Geophysical Research: Oceans*, 122(5), pp.3771-
482 3798.
- 483 Gao, L., Rintoul, S.R. & Yu, W., 2018. Recent wind-driven change in Subantarctic Mode Water
484 and its impact on ocean heat storage. *Nature Climate Change*, 8, 58.
- 485 Gent, P.R., & G. Danabasoglu 2011 Response to Increasing Southern Hemisphere Winds in
486 CCSM4, *J Climate*, 4992-4998.
- 487 Gent, P.R., Danabasoglu, G., Donner, L.J., Holland, M.M., Hunke, E.C., Jayne, S.R., Lawrence,
488 D.M., Neale, R.B., Rasch, P.J., Vertenstein, M. and Worley, P.H., 2011. The community climate
489 system model version 4. *Journal of Climate*, 24(19), pp.4973-4991.
- 490 Hasselmann, K., Sausen, R., Maier-Reimer, E. & Voss, R., 1993: On the cold start problem in
491 transient simulations with coupled atmosphere-ocean models. *Climate Dynamics*, 9, 53-61.
- 492 Hall, T.M., & T.W.N. Haine 2002: On Ocean Transport Diagnostics: The Idealized Age Tracer
493 and the Age Spectrum, *J. Phys. Ocean.*, 1987-2001.
- 494 Hogg, A. M., P. Spence, O. A. Saenko, & S. M. Downes, 2017: The energetics of Southern
495 Ocean upwelling. *J. Phys. Oceanogr.*, 47, 135–153.
- 496 Jones, D. C., T. Ito, and N. S. Lovenduski (2011), The transient response of the Southern Ocean
497 pycnocline to changing atmospheric winds, *Geophys. Res. Lett.*, 38, L15604,
498 doi:10.1029/2011GL048145.
- 499 Le Quere, C., Rödenbeck, C., Buitenhuis, E.T., Conway, T.J., Langenfelds, R., Gomez, A.,
500 Labuschagne, C.Ramonet, M., Nakazawa, T., Metzl, N. & Gillett, N. 2007 Saturation of the
501 Southern Ocean CO₂ sink due to recent climate change. *Science*, 316, 1735-1738
- 502 Marshall, J., Armour, K.C., Scott, J.R., Kostov, Y., Hausmann, U., Ferreira, D., Shepherd, T.G.
503 & Bitz, C.M., 2014. The ocean's role in polar climate change: asymmetric Arctic and Antarctic
504 responses to greenhouse gas and ozone forcing. *Phil. Trans. R. Soc. A*, 372(2019).
- 505 Roemmich, D., J Gilson, R. Davis, P. Sutton, S. Wijffels, & S. Riser, Decadal Spinup of the
506 South Pacific Subtropical Gyre, *J. Phys. Ocean.*, 37, 162-, 2007.

- 507 Roemmich, D., Gilson, J., Sutton, P. & Zilberman, N., 2016. Multidecadal change of the South
508 Pacific gyre circulation. *Journal of Physical Oceanography*, 46(6), pp.1871-1883.
- 509 Russell, J.L., Dixon, K.W., Gnanadesikan, A., Stouffer, R.J. and Toggweiler, J.R., 2006. The
510 Southern Hemisphere westerlies in a warming world: Propping open the door to the deep ocean.
511 *Journal of Climate*, 19(24), pp.6382-6390.
- 512 Sen Gupta, A., & M.H. England, 2006: Coupled Ocean–Atmosphere–Ice Response to Variations
513 in the Southern Annular Mode, *J Climate*, 19.
- 514 Sijp, W. P., & M. H. England, 2008: The effect of a northward shift in the southern hemisphere
515 westerlies on the global ocean. *Prog. Oceanogr.*, 79, 1–19
- 516 Spence, P., S. M. Griffies, M. H. England, A. M. Hogg, O. A. Saenko, & N. C. Jourdain, 2014:
517 Rapid subsurface warming and circulation changes of Antarctic coastal waters by pole- ward
518 shifting winds. *Geophys. Res. Lett.*, 41, 4601–4610
- 519 Swart, N.C. & J.C. Fyfe, 2012: Observed and simulated changes in the Southern Hemisphere
520 surface westerly wind-stress, *Geophys. Res. Lett.*, 39, L16711, doi:10.1029/2012GL052810
- 521 Tanhua, T., D. W. Waugh, & J. L. Bullister, 2013: Estimating changes in ocean ventilation from
522 early 1990s CFC-12 and late 2000s SF₆ measurements, *Geophys. Res. Lett.*, 40, 927–932,
523 doi:10.1002/grl.50251.
- 524 Thomas, M.D., De Boer, A.M., Johnson, H.L. & Stevens, D.P., 2014: Spatial and temporal
525 scales of Sverdrup balance. *Journal of Physical Oceanography*, 44, 2644-2660.
- 526 Thompson DWJ, Solomon S, Kushner PJ, England MH, Grise KM, Karoly DJ. 2011: Signatures
527 of the Antarctic ozone hole in Southern Hemisphere surface climate change. *Nat. Geosci.* 4, 471–
528 479
- 529 Ting, Y.H. & Holzer, M., 2017: Decadal changes in Southern Ocean ventilation inferred from
530 deconvolutions of repeat hydrographies. *Geophysical Research Letters*.
- 531 Waugh, D. W., F. Primeau, T. DeVries, & M. Holzer 2013 Recent changes in the ventilation of
532 the southern oceans, *Science*, 339, 568.
- 533 Waugh, D.W. (2014). Changes in the ventilation of the southern oceans, *Philosophical*
534 *Transactions A.*, 373, 0130269.
- 535 Waugh, D.W., A. Mc C. Hogg, P Spence, M. H. England, T. W.N. Haine, 2019: Response of
536 Southern Ocean ventilation to changes in mid-latitude westerly winds, *J Climate*, 32, 5345-5361.
- 537
- 538



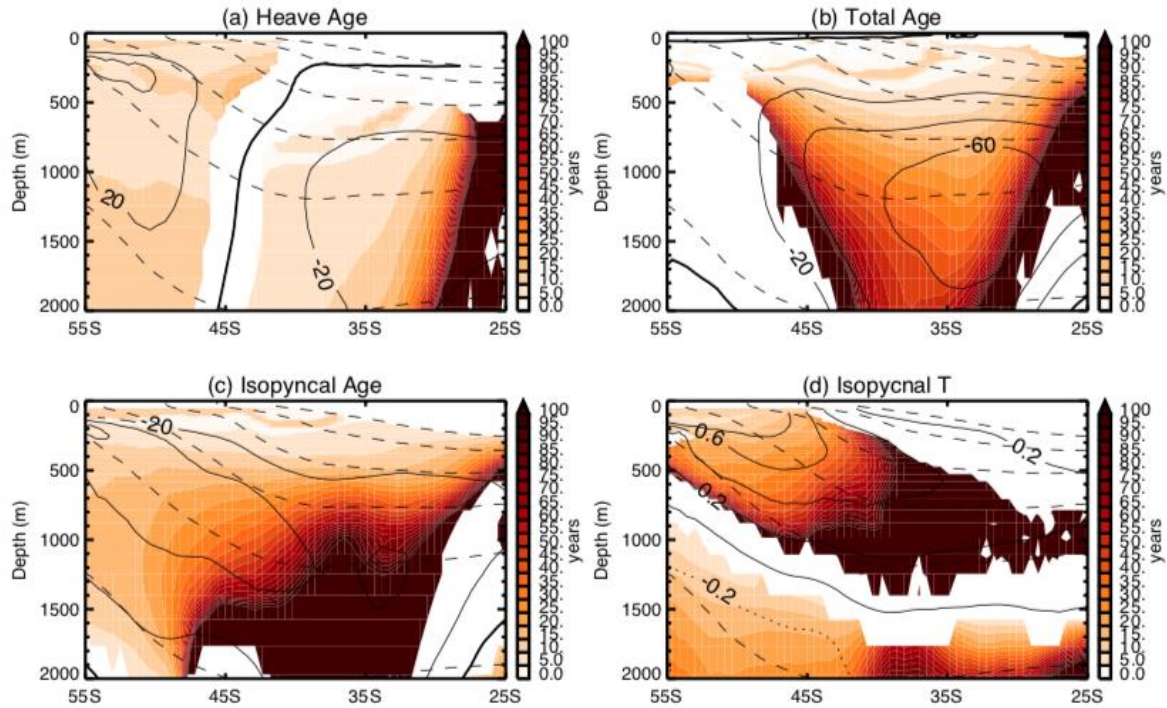
539

540 Figure 1: (a) Latitudinal variations of the time-mean zonal-mean zonal wind stress for the Control and Perturbation
 541 simulations. (b) Map of barotropic stream function, and latitude-height plots of zonal-mean (c) σ_2 , (d) total, (e)
 542 heave, (f) isopycnal change in age, (g) T, and (h) S. Shading shows response (Perturbation-Control) at year 100
 543 (with the heavy black contour showing zero response), solid contours show for Control simulations at year 100, and
 544 dashed contours show isopycnal surfaces $\sigma_2 = 33.5, 34.0, \dots 37.0 \text{ kg/m}^3$.



545

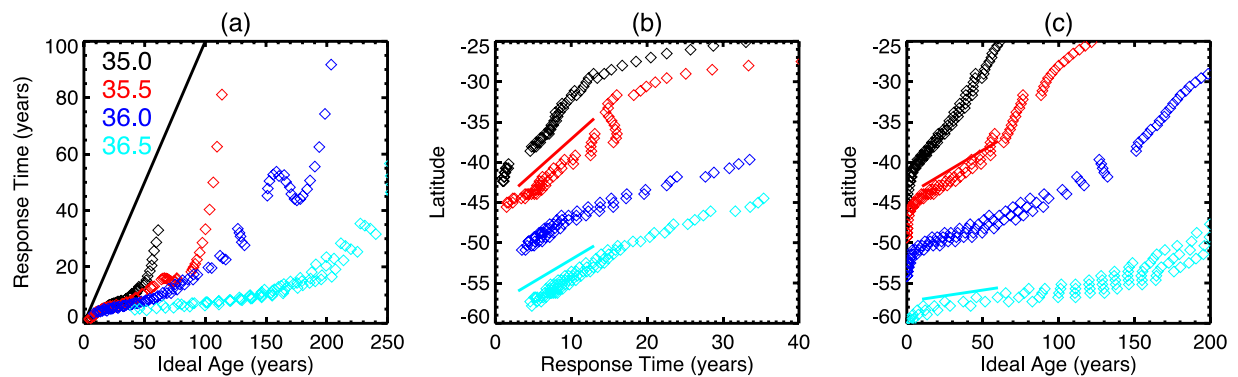
546 Figure 2: Time series of change in (a) minimum BSF in Pacific, Indian, and Atlantic oceans,
 547 (b) potential density, (c) age, (d) heave age, (e) isopycnal age, and (f) isopycnal T. (b)-(f)
 548 show zonal-mean values 49°S, 200m, 43°S, 640m, and 36°S, 790m, which all lie on the $\sigma_2=36$
 549 kg/m^3 surface (see diamonds in Fig 1). Dashed curves show fit using equation (1), and
 550 corresponding response time τ is listed above curves.



551

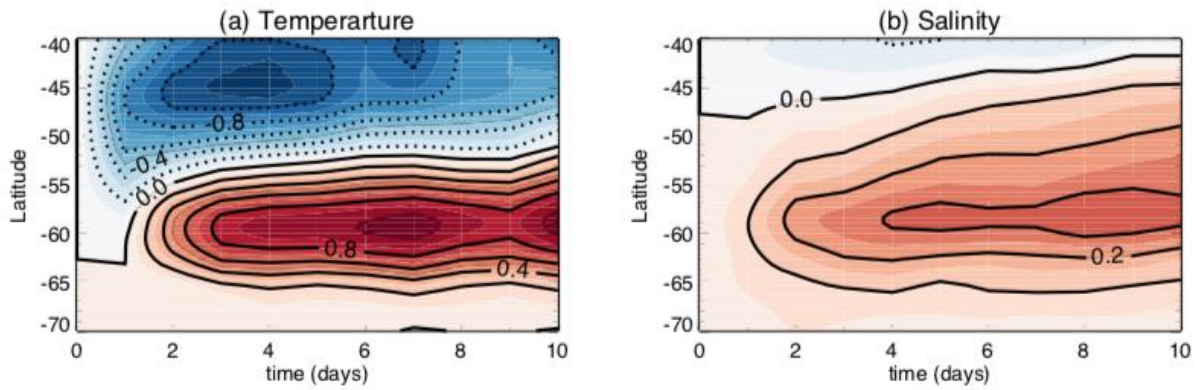
552 Figure 3: Latitude-height plots of response time τ for (a) potential density and heave change in
 553 age, (b) total change in age, (c) isopycnal change in age, and (d) isopycnal change in T and S.
 554 Solid contours show response (Perturbation-Control) at year 100 and dashed contours show
 555 isopycnal surfaces $\sigma_2 = 33.5, 34.0, \dots 37.0 \text{ kg/m}^3$.

556

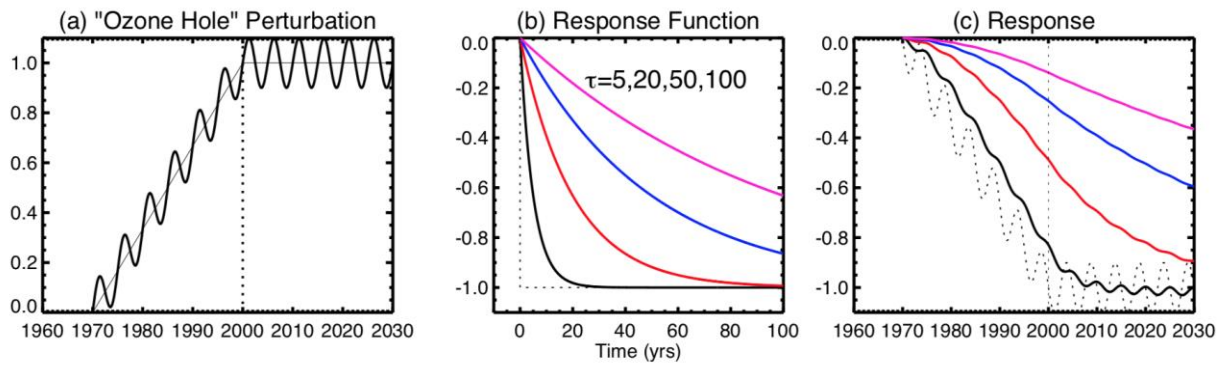


557

558 Figure 4: Variation of (a) response time and (b) ideal age with latitude, for 35, 35.5, 36.0, and
 559 36.5 kg/m^3 isopycnal surfaces. Solid lines correspond to linear latitude-time relationships with
 560 slopes of 0.2 cm/s (blue) and 0.3 cm/s (red) in panel (a), and of 0.01 cm/s (blue) and 0.04 cm/s
 561 (red) in panel (b). (c) Variation of response time of ideal age with ideal age for same isopycnal
 562 surfaces as in (a) and (b).



563
 564 Figure 5: Temporal evolution of anomalies in zonal-mean (a) temperature and (b) salinity at 5m.
 565 Anomalies are deviations from initial values.
 566



567
 568 Figure 6: (a) wind stress perturbation mimicking changes due to ozone depletion and
 569 stabilization, (b) response functions (R) given by equation 1 with $\tau = 5, 20, 50,$ and 100 yrs, and
 570 (c) response to perturbation (a) for $R(t)$ shown in (b). All fields normalized.
 571

572